Applied Chemical Engineering (2025) Volume 8 Issue 3 ISSN: 2578-2010 (O)
doi: 10.59429/ace.v8i3.5637

ORIGINAL RESEARCH ARTICLE

Eco-friendly iron removal from contaminated water using chemically modified rice straw: Adsorption mechanisms and performance

Nur Qudus[1*], Harianingsih[2], Virgiawan Adi Kristianto[1], Dimas Gustoro[1], Muhammad Arief Kariem[3], Indra Sakti Pangestu[2], Rizky Ilham Fadzillah[2]
[1] Department of Civil Engineering, Faculty of Engineering, Universitas Negeri Semarang, Kampus Sekaran Gunungpati, Semarang 50229, Indonesia
[2] Department of Chemical Engineering, Faculty of Engineering, Universitas Negeri Semarang, Kampus Sekaran Gunungpati, Semarang 50229, Indonesia
[3] Department of Chemical Engineering, Faculty of Engineering, Universitas Muhammadiyah Palembang, Talang Banteng Street 13, Ulu Palembang, Indonesia
*** Corresponding author:** Nur Qudus, nurqudus@mail.unnes.ac.id

ABSTRACT

The availability of water does not always guarantee its quality, particularly when it is contaminated with iron (Fe), which poses health risks such as kidney failure, cardiovascular diseases, and digestive disorders. This study evaluates the potential of rice straw -modified $Ca(OH)_2$ (Rs-OCa) as an adsorbent for removing Fe(II) ions from groundwater. Rice straw, a widely available agricultural waste in Indonesia, was chemically modified to enhance its adsorption capacity by increasing active sites, removing lignin, and improving its affinity for metal ions. FTIR analysis confirmed the presence of hydroxyl (-OH) and carboxyl (-COOH) functional groups, while XRD analysis revealed both crystalline and amorphous structures that contribute to stability and adsorption efficiency. Adsorption tests indicated optimal Fe(II) removal at pH 4–5 with an adsorbent dose of 0.75 g per 100 mL of solution. The adsorption isotherm followed the Langmuir model, with a maximum adsorption capacity (Q_m) of 22.47 mg/g, indicating a homogeneous monolayer adsorption mechanism. The Freundlich model (KF = 8.91 mg/g, n = 2.5) further confirmed surface heterogeneity and high adsorption efficiency at low Fe (II) concentrations.The results demonstrate that Rs-OCa is an effective, economical, and environmentally friendly adsorbent for iron removal from contaminated water.

Keywords: adsorption mechanism; agricultural waste; contaminated water; iron removal; rice straw

ARTICLE INFO

Received: 15 July 2025
Accepted: 31 July 2025
Available online: 20 August 2025

1. Introduction

Abundant water availability does not always guarantee clean water quality that meets established standards[1]. In Indonesia, concerns over the presence of iron (Fe) in drinking water have been increasingly reported, with several regions recording Fe concentrations exceeding the recommended thresholds[2]. According to national standards, the permissible limit for total Fe content in drinking water is 0.3 mg/L[3]. Iron contamination in groundwater typically exists in the form of soluble Fe (II) (ferrous ions), which, upon exposure to atmospheric oxygen or dissolved oxygen in water, undergoes oxidation to form Fe (III) (ferric ions). The ferric ions readily hydrolyze and precipitate as reddish-brown suspended solids, such as $Fe(OH)_3$, contributing to aesthetic and operational issues in water systems. While the initial concern often centers on the removal of soluble Fe (II), the presence of Fe (III) in the form of suspended solids also poses a significant challenge, as it can clog pipelines, stain surfaces, and reduce water clarity. Therefore, effective treatment methods should address both the

removal of soluble iron and its oxidized particulate forms. According to the World Health Organization (WHO), the recommended limit for total iron (Fe (II)/Fe (III)) in drinking water is 0.3 mg/L due to its potential to cause organoleptic problems and, at higher levels, adverse health effects such as gastrointestinal disturbances. In contrast, several groundwater sources in iron-rich regions of Indonesia have been reported to contain total iron concentrations exceeding 1.0 mg/L, far above this threshold. This highlights the urgent need for effective, sustainable, and low-cost iron removal strategies—especially those capable of targeting both dissolved and precipitated iron species—to ensure safe drinking water and compliance with national and international water quality standards.

While iron is an essential element for human health, playing a role in enzymatic oxidation processes and the formation of respiratory pigments such as hemoglobin[4], excessive levels can pose serious health risks. High concentrations of Fe in drinking water have been associated with digestive disorders, kidney dysfunction, poisoning, cancer[5], and cardiovascular diseases through the promotion of arterial plaque formation leading to atherosclerosis[6]. Prolonged consumption of Fe-contaminated water may significantly increase the risk of chronic diseases, making the issue a critical public health concern. To address heavy metal contamination, various water treatment methods have been developed. Among these methods, ceramic membrane filtration[7], coagulation-flocculation processes[8], and phytoremediation using aquatic plants have been widely applied[9]. Despite their effectiveness, these methods often face challenges related to high operational costs, maintenance complexity, and limited long-term sustainability. Consequently, there has been growing interest in alternative water treatment strategies that are more cost-effective, sustainable, and environmentally friendly. Bioadsorption has emerged as one of the promising alternatives due to its low cost, eco-friendliness, and reusability of materials[10]. Particularly, the use of agricultural waste products as bioadsorbents aligns with sustainable development goals by promoting waste valorization. Modified biopolymers, such as treated agricultural byproducts, have shown notable potential as effective adsorbent materials. One such material is rice straw (Rs), an abundant agricultural residue generated extensively in rice-producing countries like Indonesia. Indonesia alone produces millions of tons of rice straw annually, much of which remains underutilized and is often burned or left to decompose, contributing to air pollution, CO_2 emissions, and the greenhouse effect[11].

Rice straw primarily consists of lignin, cellulose, and hemicellulose. Its high lignin content, however, limits its natural adsorption capacity for heavy metals, including Fe(II) ions[12]. Chemical modification is required to enhance its adsorption properties. One effective method involves treating rice straw with calcium hydroxide ($Ca(OH)_2$), which alters its chemical structure by increasing the abundance of hydroxyl (-OH) and carboxyl (-COOH) functional groups while simultaneously reducing lignin content. These changes facilitate stronger interactions between the adsorbent and Fe(II) ions, thereby improving the material's overall adsorption capacity. Although conventional techniques such as ceramic membranes, coagulation-flocculation, and phytoremediation have been explored extensively, questions remain regarding their cost-efficiency, practicality, and scalability, particularly in rural or low-income settings. Bioadsorption offers a compelling alternative; however, existing bioadsorbents often suffer from limited adsorption efficiency and lack optimization for heavy metal removal. Research into the development and application of modified agricultural waste-based adsorbents remains insufficient, particularly concerning Fe(II) ion removal.The potential use of $Ca(OH)_2$-modified rice straw (referred to as Rs-OCa) represents a promising solution. Nevertheless, comprehensive studies evaluating its adsorption capacity, stability, and operational parameters under real-world conditions are scarce. Critical parameters such as solution pH, adsorbent dosage, and contact time need to be systematically investigated to optimize the removal efficiency of Fe(II) ions. Addressing these gaps is essential for advancing the practical application of bioadsorption techniques in water treatment and for promoting sustainable environmental management practices in regions heavily burdened by agricultural waste and water quality issues.

Based on the background described, this study aims to evaluate the effectiveness of $Ca(OH)_2$-modified rice straw (Rs-OCa) as an adsorbent for Fe(II) removal from aqueous solutions. The study focuses on the characterization of the modified adsorbent and examines the influence of key operational parameters, including solution pH and adsorbent dosage, on the Fe(II) adsorption process. The findings are expected to contribute valuable insights into the development of affordable, efficient, and sustainable water treatment technologies.

2. Materials and methods

2.1. Material

The main materials in this study include rice straw waste (Rs), the reagents used include $Fe(NO_3)_2 \cdot H_2O$ Merck 1.03943, H_2SO_4 Merck 1.00731, distilled water, and $Ca(OH)_2$ Merck 1.02047. The equipment used in this study includes Atomic Absorption Spectrophotometer (AAS), furnace, oven, desiccator, 80 mesh sieve, blender, pH meter, analytical balance, stand, clamp, and chromatography column. The analytical instruments used in this study include FTIR (Fourier Transform Infrared Spectrometer): Perkin Elmer, XRD (X-Ray Diffraction): Panalytical X'Pert 3 Powder.

2.2. Procedure

The synthesis and application of rice straw-originated calcium-modified adsorbent (Rs-OCa) were successfully carried out, as illustrated in **Figure 1**. The process involved the preparation of raw rice straw, followed by drying, thermal treatment, and chemical modification using $Ca(OH)_2$ to enhance its adsorption capacity. The resulting modified adsorbent was subsequently tested for its effectiveness in removing Fe(II) from aqueous solutions under varying pH conditions and adsorbent dosages. The synthesized Rs-OCa exhibited notable adsorption performance, with its effectiveness significantly influenced by both solution pH and the quantity of adsorbent applied. The adsorption study indicated that Fe(II) removal efficiency increased with rising pH levels, reaching an optimum point before declining due to the precipitation of hydroxide ions. Moreover, variation in the adsorbent dosage demonstrated that a specific mass resulted in the highest Fe(II) uptake, suggesting the existence of an optimal number of available active sites on the adsorbent surface. To gain further insights into the physicochemical properties of the synthesized Rs-OCa, Fourier-transform infrared spectroscopy (FTIR) and X-ray diffraction (XRD) analyses were performed. These characterizations confirmed the presence of functional groups and crystalline structures that contribute to the adsorption mechanism. Additionally, pH and water hardness measurements were conducted to evaluate the quality of the treated water after the adsorption process, ensuring the feasibility of Rs-OCa as a practical material for Fe(II) removal in real-world applications. The following sections present a comprehensive discussion of the structural characteristics and adsorption performance of Rs-OCa, supported by spectral and analytical evidence.

Figure 1. Rs-Oca development and characterization procedure.

2.2.1. Modification of rice straw with $Ca(OH)_2$

Prior to the modification process, rice straw was thoroughly washed and cut into small pieces to facilitate drying. The samples were subsequently oven-dried at 105 °C for 2 hours until completely dehydrated. The dried rice straw was heated in a muffle furnace at 500 °C for 1 hour to induce structural modification, rather than for conventional biochar production. This treatment was intended to enhance the porosity and surface characteristics of the raw material while preserving much of its native lignocellulosic composition. Following carbonization, the rice straw was crushed and sieved through an 80-mesh screen to obtain a uniform particle size. Subsequently, 100 grams of rice straw (Rs) were immersed in a 0.1 M NaOH solution for 24 hours. This pretreatment was intended to remove lignin from the rice straw matrix, thereby enhancing its adsorption capacity. After the soaking process, the solution was decanted, and the Rs samples were neutralized and oven-dried at 105 °C until the moisture content fell below 10%.

For the chemical modification, the dried rice straw was mixed with $Ca(OH)_2$ in a 1:1 weight ratio to produce a modified adsorbent referred to as Rs-OCa. The mixture was stirred at 200 rpm using a magnetic stirrer for 5 hours. Upon completion, the suspension was decanted to achieve a neutral pH, filtered, and subsequently dried.Separately, 3.5 grams of $Fe(NO_3)_2 \cdot H_2O$ were dissolved in 100 mL of distilled water, followed by the addition of a few drops of 0.1 M H_2SO_4. The solution was then diluted with distilled water to a final volume of 1 liter.

2.2.2. Characterization of pH and adsorbent mass on Fe (II) adsorption by Rs-OCa

To evaluate the influence of pH on adsorption performance, 25 mL of Fe(II) solution with a concentration of 50 ppm was prepared in separate containers at varying pH levels of 2, 3, 4, 5, 6, 7, and 8. The pH adjustments were carried out using 0.1 M H_2SO_4 and 0.1 M NaOH to maintain stability throughout the adsorption process. Subsequently, 0.75 grams of crushed Rs-OCa were added to each solution, and the adsorption capacity was determined using atomic absorption spectroscopy (AAS). To investigate the effect of adsorbent mass, Rs-OCa samples weighing 0.25, 0.5, 0.75, 1.0, and 1.25 grams were introduced into an ion-exchange chromatography

column. Thereafter, 25 mL of Fe(II) solution at a concentration of 50 ppm and pH 4 were passed through the column, and the resulting adsorption capacity was analyzed by AAS.

2.3. Analysis

2.3.1. FTIR and XRD analysis

Rs-OCa was mixed with KBr at a 1:100 ratio and then pressed into transparent pellets using a press. The sample mixture was placed between transparent KBr plates. The wavelength range was set to 4000–400 cm^{-1}. The sample was then scanned using FTIR to obtain the infrared spectra. For XRD analysis, the sample was ground into a fine powder to ensure random particle orientation. If using a thin film or bulk material, the sample was placed directly on the sample holder without grinding. Diffractometer Settings: Angular range (2θ), Scan rate (degrees per minute), X-ray wavelength (λ = 1.5406 Å).

2.3.2. Langmuir and freundlich isothermal adsorption

After preparation and adjustment to pH 4.00, 25 mL of Fe(II) solution with a concentration of 50 ppm was passed through the chromatography column for five minutes. The amount of Fe(II) ions adsorbed was then measured using an Atomic Absorption Spectrophotometer (AAS) after the adsorption process was completed. Subsequently, the data were computed and analyzed graphically using the Langmuir equation (1) and the Freundlich equation (2)[12]:

$$\frac{C_e}{Q_e} = \frac{C_e}{Q_m} + \frac{1}{Q_m K_L} \quad (1)$$

$$log\ Q_e = \left(\frac{1}{n}\right) \ln C_e + log\ K_F \quad (2)$$

Ce is the adsorbate concentration in solution at equilibrium (mg/L), Qe is the equilibrium adsorption capacity (mg/g). Maximum adsorption capacity (mg/g) is denoted by Qm. KL is the L/mg, the Langmuir constant. Kf is the Freundlich model's adsorption capacity. The heterogeneity of the adsorbent surface is indicated by n = adsorption intensity. Ce is the adsorbate concentration in solution (mg/L) following adsorption. Qe is the equilibrium adsorption capacity (mg/g).

3. Results and discussion

3.1. Effect of pH on Fe (II) adsorption by Rs-OCa

pH plays a critical role in the adsorption process, as it influences both the surface charge of the adsorbent and the speciation of Fe(II) ions in solution[13]. The experimental results show that adsorption capacity increases with pH, reaching an optimum at pH 4–5. At lower pH values (<3), an excess of H^+ ions competes with Fe(II) for the active binding sites on the adsorbent, leading to lower removal efficiency. In contrast, at pH values above 6, Fe(II) begins to precipitate as $Fe(OH)_2$, which reduces its availability for adsorption[14].

At low pH, the protonation of functional groups such as -OH and -COOH occurs:

$$\text{-OH} + H^+ \rightarrow \text{-}OH_2^+ \quad (3)$$

$$\text{-OH} + H^+ \rightarrow \text{-}OH_2^+ \quad (4)$$

These protonated sites generate a net positive surface charge, resulting in electrostatic repulsion between the adsorbent and positively charged Fe(II) ions, thereby lowering adsorption efficiency[15]. As pH increases to 4–5, this competition is reduced, enabling more Fe(II) ions to bind. Adsorption in this range can occur through mechanisms such as ionic complexation and hydrogen bonding[16–18].

At neutral to basic pH, deprotonation occurs:

$$\text{-}COO^- + H^+ \rightarrow \text{-COOH} \quad (5)$$

$$-COO^- + H^+ \rightarrow -COOH \quad (6)$$

pH plays a critical role in the adsorption process as it influences both the surface charge of the adsorbent and the behavior of metal ions in the solution[13]. Experimental findings indicate that adsorption capacity improves with increasing pH, reaching an optimal range at pH 4–5. At very low pH levels (pH < 3), an excess of H^+ ions in the solution competes with Fe(II) ions for binding to the active sites of the adsorbent, resulting in lower adsorption efficiency. Conversely, at pH levels above 6, Fe(II) ions begin to precipitate as $Fe(OH)_2$, reducing adsorption effectiveness because Fe(II) is no longer in a dissolved state[14].

This makes the surface negatively charged. However, beyond pH 6, Fe(II) forms hydroxide species such as $FeOH^+$, $Fe(OH)_2$, and $[Fe(OH)_4]^{2-}$, which are less readily adsorbed. Although Rs-OCa contains $Ca(OH)_2$ and can raise solution pH, the material still functions effectively by binding Fe(II) before significant precipitation occurs. Additionally, pretreatment steps can maintain the pH within the optimum range for adsorption. This highlights the importance of pH control in practical applications.

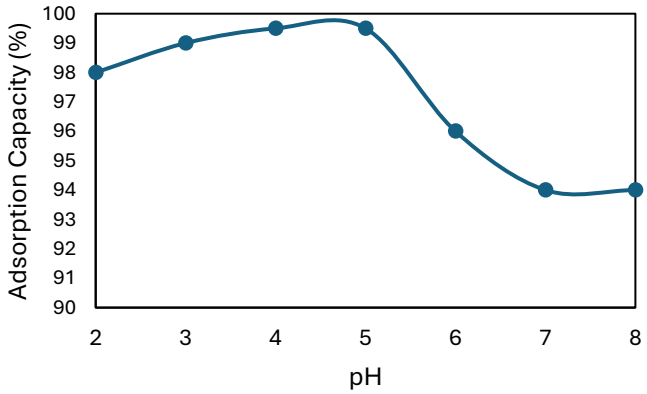

Figure 2. Adsorption capacity of Rs-OCa at varying pH levels.

Based on **Figure 2**, at low pH, the adsorbent surface tends to become positively charged due to protonation. This occurs because active functional groups on the adsorbent, such as carboxyl (-COOH), hydroxyl (-OH), and amine ($-NH_2$), accept protons (H^+) in acidic conditions, resulting in a positively charged adsorbent[15]. With the presence of a positive charge on the adsorbent surface, electrostatic repulsion occurs between the adsorbent surface and Fe(II) ions, which are also positively charged. In theory, this condition is unfavorable for the adsorption of cations such as Fe(II) because electrostatic interactions tend to be weak[16]. At extremely low pH (pH < 3), the solution contains an abundance of H^+ ions, leading to strong competition between H^+ and Fe(II) for active sites on the adsorbent surface. However, as the pH increases slightly to 4–5, the H^+ ion concentration decreases, making it easier for Fe(II) to bind to the active sites of the adsorbent[17]. In addition to electrostatic interactions, Fe(II) adsorption can also occur through specific interactions, such as hydrogen bonding, complexation, or ion exchange mechanisms. The carboxyl group (-COOH), which has undergone protonation, can still interact with Fe(II) ions through ionic complexation mechanisms, thereby enhancing adsorption efficiency[18]. At neutral to basic pH, Fe(II) adsorption efficiency decreases due to several key factors. At high pH, the adsorbent surface tends to become negatively charged due to deprotonation. For example, the hydroxyl group (-OH) loses its proton, forming a negatively charged ($-O^-$) group[19]:

$$-OH \rightarrow -O^- + H^+ \quad (7)$$

$$-OH \rightarrow -O^- + H^+ \quad (8)$$

Likewise with the carboxyl group (-COOH), which will change to $-COO^-$[20]:

$$-COOH \rightarrow -COO^- + H^+ \quad (9)$$

$$-COOH \rightarrow -COO^- + H^+ \quad (10)$$

As a result of this change, electrostatic repulsion occurs between Fe(II) cations and the negatively charged adsorbent surface, leading to a reduction in adsorption efficiency. In an adsorption system based on electrostatic interactions, this condition is highly unfavorable, as metal ions tend to be repelled from the adsorbent surface. At higher pH levels (above pH 6.0), Fe(II) ions undergo hydrolysis, forming various metal ion species that differ from the Fe^{2+} form initially present in the solution. Some of the Fe(II) species formed include[21]:

$$Fe^{2+} + OH^- \rightarrow FeOH^+ \quad (11)$$

$$Fe^{2+} + OH^- \rightarrow FeOH^+ \quad (12)$$

$$FeOH^+ + OH^- \rightarrow Fe(OH)_2 \quad (13)$$

$$FeOH^+ + OH^- \rightarrow Fe(OH)_2 \quad (14)$$

$$Fe(OH)_2 + OH^- \rightarrow [Fe(OH)_4]^{2-} \quad (15)$$

$$Fe(OH)_2 + OH^- \rightarrow [Fe(OH)_4]^{2-} \quad (16)$$

The formation of $FeOH^+$, $Fe(OH)_2$, or $[Fe(OH)_4]^{2-}$ complex species reduces the direct interaction between Fe(II) ions and the adsorbent surface. Under these conditions, Fe(II) ions are more likely to precipitate or form $Fe(OH)_2$ deposits, meaning they are no longer in a soluble form that can be adsorbed onto the adsorbent surface[22]. Additionally, under alkaline pH conditions, certain organic-based adsorbents, such as $Ca(OH)_2$-modified rice straw or modified orange peel, can undergo degradation, further reducing their overall adsorption capacity[23].

3.2. Effect of adsorbent mass on Fe (II) adsorption by Rs-OCa

Adsorption performance was observed to increase with the mass of Rs-OCa up to an optimal range (0.75–1.0 g per 100 mL solution). Beyond this range, further increases in adsorbent mass did not significantly enhance Fe(II) removal[24]. This is likely due to the saturation of available Fe(II) ions, resulting in unused active sites.At higher adsorbent doses, agglomeration may occur, decreasing the effective surface area[28]. Additionally, since Rs-OCa contains alkaline components ($Ca(OH)_2$), excessive dosage can raise solution pH, which may promote Fe(II) hydrolysis and reduce adsorption efficiency[23].

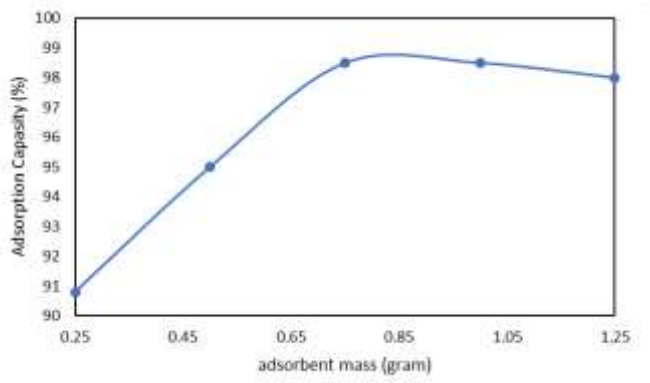

Figure 3. Effect of Rs-OCa dosage on Fe(II) adsorption capacity.

Based on **Figure 3**, increasing the amount of adsorbent allows more Fe(II) ions to be captured, as more active sites become available. However, beyond a certain point, adding more adsorbent no longer enhances adsorption efficiency. This occurs because the adsorbent surface reaches its maximum capacity and becomes saturated with Fe(II) ions[25].

When adsorbent is introduced into a solution containing Fe(II) ions, the number of active sites—such as carboxyl (-COOH), hydroxyl (-OH), and amine (-NH_2) groups—also increases. These functional groups, which contain free electron pairs, attract positively charged metal ions (cations) through electrostatic interactions and complexation mechanisms[26]. Once all available sites are occupied, adsorption ceases to increase, even if additional adsorbent is added.

At high Fe(II) concentrations, the active sites become occupied quickly, leaving no available space for additional Fe ions to bind. Conversely, if the adsorbent amount is increased without a proportional increase in Fe(II) concentration, some of the adsorbent remains inactive, thereby reducing overall efficiency. Similarly, when Fe(II) concentration is too low, adding extra adsorbent has little effect, as there are insufficient Fe ions to interact with all available active sites[27].

Excessive use of adsorbent can also lead to particle agglomeration, where adsorbent particles clump together, reducing the effective surface area and consequently lowering adsorption efficiency[28]. In biomaterial-based adsorbents such as $Ca(OH)_2$-modified rice straw, increasing the adsorbent mass can also raise the solution's pH. At high pH levels, Fe(II) ions may undergo hydrolysis, forming species such as $FeOH^+$, $Fe(OH)_2$, and $Fe(OH)_3$, which are less readily adsorbed onto the adsorbent surface.

Although the experimental design of this study successfully illustrates the adsorption mechanism of Fe(II) onto $Ca(OH)_2$-modified rice straw (Rs-OCa) under controlled laboratory conditions, it is important to consider that actual groundwater environments are significantly more complex. In real-world applications, the adsorbent would likely encounter additional challenges, including the presence of fine suspended particles, competing soluble metal ions such as Mn^{2+}, Mg^{2+}, K^+, and Na^+, as well as negatively charged species such as carbonate (CO_3^{2-}), sulfate (SO_4^{2-}), and nitrate (NO_3^-). These coexisting substances can compete with Fe(II) ions for adsorption sites, potentially reduce available active sites, alter surface charge interactions, and even promote fouling or blockage of the adsorbent pores. As a result, the overall adsorption efficiency for Fe(II) could be diminished when Rs-OCa is applied in untreated groundwater systems.

3.3. FTIR spectrum analysis of Rs and Rs-Oca

FTIR analysis was conducted to investigate functional group changes before and after modification. Both Rs and Rs-OCa displayed broad bands at 3200–3500 cm^{-1}, indicating -OH stretching[29,30]. A reduction in peak intensity for Rs-OCa suggests partial consumption of hydroxyl groups due to reaction with $Ca(OH)_2$ and possible dehydration during treatment[31]. C–H stretching around 2900–3000 cm^{-1} corresponds to lignin structures, and reduced intensity in Rs-OCa implies partial breakdown of organic components[32]. Increased peak intensity at 1700 cm^{-1} (C=O stretching) in Rs-OCa indicates enhanced carboxylic functionality, which improves Fe(II) binding via complexation[33,34]. The 1200–1000 cm^{-1} range reflects C–O and Si–O vibrations from cellulose and hemicellulose. The enhancement in Rs-OCa implies increased oxygen-containing groups due to surface modification[35,36].

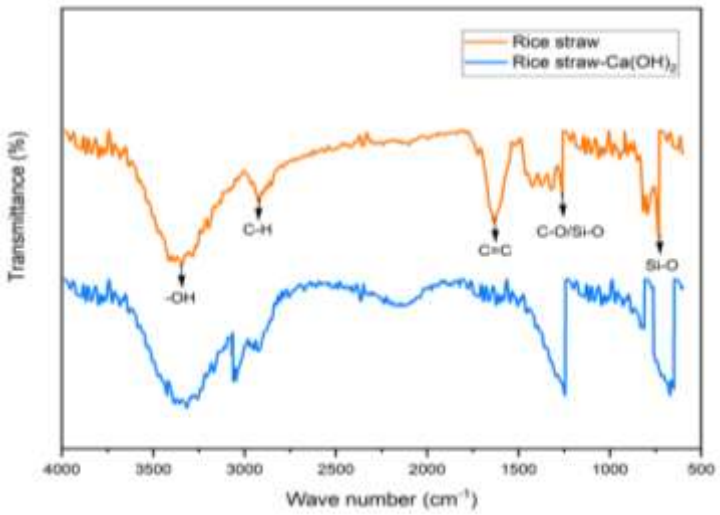

Figure 4. FTIR spectra comparison of raw rice straw (Rs) and modified rice straw (Rs-OCa).

Based on **Figure 4**, both rice straw and rice straw-Oca exhibit a broad peak in the 3200–3500 cm^{-1} range, indicating the presence of hydroxyl (-OH) groups[29]. The presence of hydroxyl (-OH) groups highlights the hydrophilic nature of Rs-OCa, which plays a crucial role in adsorption by serving as active sites that attract metal ions such as iron[30]. In terms of intensity, the peak in the first spectrum is lower than in the second spectrum, suggesting a reduction in the number of hydroxyl groups. This decrease may be attributed to the chemical modification of rice straw, particularly its interaction with $Ca(OH)_2$, which diminishes the prominence of -OH groups. Additionally, dehydration during processing could have removed some of the bonded water[31].

Small peaks observed in the 2900–3000 cm^{-1} range correspond to aliphatic C-H stretching. These peaks confirm the presence of organic components, such as lignin or other carbon-based structures, which are commonly found in biomaterial-based adsorbents[32]. In terms of intensity, the second spectrum displays a smaller peak, indicating possible degradation or alteration of aliphatic substances, such as lignin or hemicellulose, during modification. A strong signal around 1700 cm^{-1} signifies the presence of C=O groups, which could originate from carboxylic acids (-COOH), esters, ketones, or other carbonyl-containing compounds[33]. The C=O group contributes to the material's polar characteristics, enhancing its ability to interact with metal ions through complexation mechanisms. Notably, the higher intensity in the second spectrum suggests increased reactivity of the carbonyl group, likely due to surface modifications, such as oxidation during heating or the formation of additional carboxyl (-COOH) groups. A peak near 1600 cm^{-1} is associated with aromatic C=C stretching or double bonds, commonly found in lignin or other aromatic structures[34]. These groups indicate the material's rigid and stable structure, typical of biomaterials or polymers. However, the lower intensity of this peak in the second spectrum suggests the breakdown of aromatic structures, possibly due to chemical modifications, such as treatment with $Ca(OH)_2$. Another peak in the 1200–1000 cm^{-1} range corresponds to C-O or Si-O stretching, depending on the material type[35]. This peak is typically linked to polysaccharides, such as cellulose or hemicellulose. The carboxyl (-COOH) group, which is crucial for metal ion interactions, is also indicated by this peak. The higher intensity of this peak in the second spectrum suggests an increase in carboxyl or other oxygen-containing functional groups, enhancing the material's reactivity toward Fe(II) ions[36].

In summary, FTIR analysis reveals several key characteristics of the material: The presence of hydroxyl (-OH) groups, which are essential for adsorption and demonstrate hydrophilic properties. The presence of carbonyl (C=O) and carboxyl (-COOH) groups, which facilitate metal ion interactions through complexation mechanisms. Organic components such as lignin, cellulose, or hemicellulose, confirming the material's biomass origin[37].

3.4. XRD analysis of Rs-Oca

XRD analysis revealed a combination of crystalline and amorphous structures in Rs-OCa. The semi-crystalline nature supports mechanical strength and structural stability, while the amorphous components (from lignin and cellulose) provide abundant active sites for adsorption[38,39]. The presence of $Ca(OH)_2$ in Rs-OCa was also confirmed by characteristic peaks, which contribute additional hydroxyl groups that facilitate Fe(II) binding. The dual-phase nature (crystalline + amorphous) of Rs-OCa enhances both durability and adsorption efficiency[40]. Additionally, the stability of the crystalline phase supports regeneration and reuse of the adsorbent under various conditions[41].

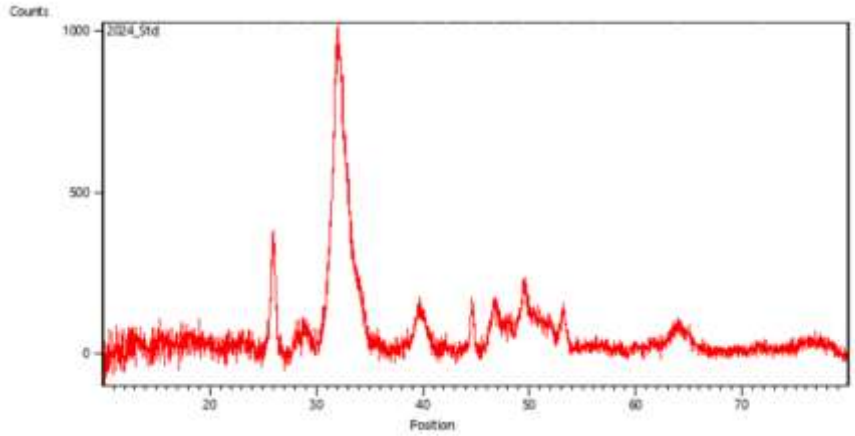

Figure 5. X-ray diffraction (XRD) pattern of $Ca(OH)_2$-modified rice straw (Rs-OCa).

Based on **Figure 5**, rice straw exhibits strong structural stability due to its crystalline phase, which helps maintain its adsorption efficiency over time. The hydroxyl (-OH) groups and other active functional groups on the surface of the crystalline phase play a crucial role in attracting Fe(II) ions through chemical processes such as ion exchange or complexation[38]. The XRD pattern reveals the presence of semi-crystalline or amorphous components, indicated by a diffuse background diffraction pattern across the 2θ range of 20° to 50°. These amorphous phases often originate from organic materials, such as lignin, cellulose, or hemicellulose, which are essential for the adsorption process[39]. The amorphous structure of Rs-OCa provides more active sites and pores, enhancing its interaction with Fe(II) ions through mechanisms such as complexation with carbonyl groups (-C=O), physical adsorption, and electrostatic interactions with negatively charged surfaces. The combination of a stable crystalline phase and a reactive amorphous phase gives Rs-OCa a high adsorption capacity and fast kinetics, particularly in solutions with low to moderate Fe(II) ion concentrations[40]. The adsorption performance of Rs-OCa is further enhanced through modification with inorganic compounds like $Ca(OH)_2$, which introduces additional hydroxyl groups, creating extra active sites and improving the material's ability to interact with Fe(II) ions. Additionally, the crystalline phase increases Rs-OCa's resistance to physical and chemical degradation during adsorption, enabling the material to be reused after regeneration. The structural stability provided by the crystalline phase ensures consistent adsorption performance across various operating conditions, including acidic to neutral pH levels[41]. The XRD pattern of Rs-OCa highlights the functional advantages of combining crystalline and amorphous phases. While the crystalline phase ensures mechanical and chemical stability, the amorphous phase contributes a large specific surface area and heterogeneous active sites, further enhancing adsorption efficiency. In summary, these findings confirm that Rs-OCa is an effective adsorbent for Fe(II) ions[42].

3.5. Fe(II) adsorption isotherm analysis

Fe(II) adsorption by Rs-OCa was evaluated using the Langmuir and Freundlich models. The Langmuir model yielded a high correlation coefficient (R^2 = 0.9997), indicating monolayer adsorption on a uniform

surface with a maximum adsorption capacity (Q_m) of 22.47 mg/g and a Langmuir constant (K_l) of 0.1539 L/mg[42].

The Freundlich model showed K_F = 8.91 mg/g and n = 2.5, suggesting favorable adsorption on heterogeneous surfaces at low concentrations. Although both models were applicable, the Langmuir model provided a better fit, confirming the uniformity of Rs-OCa active sites and the saturation limit of Fe(II) adsorption.

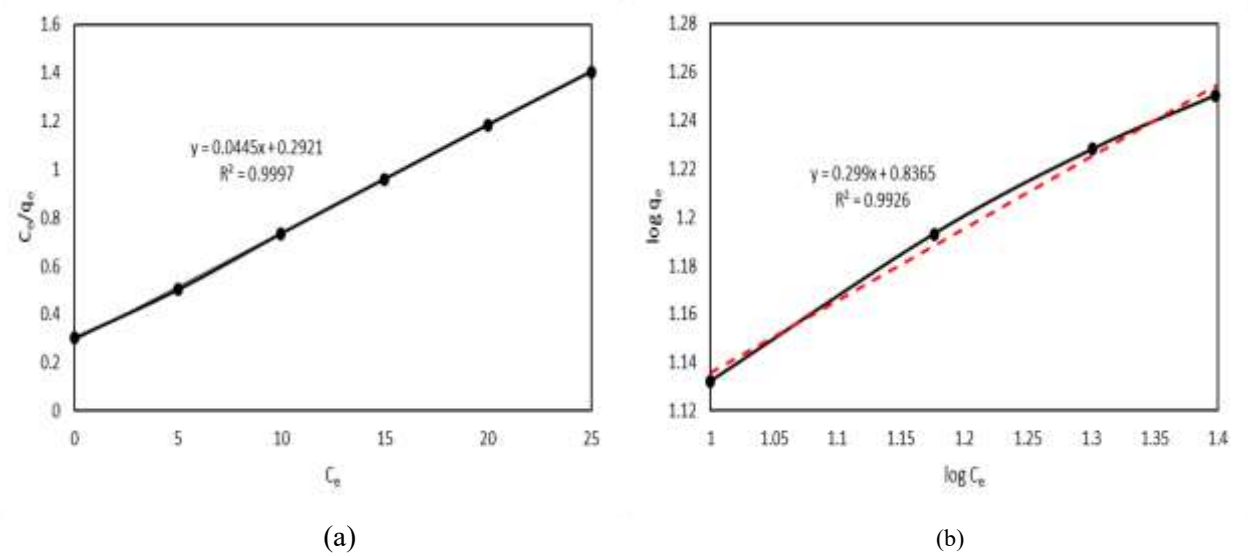

(a) (b)

Figure 6. Adsorption isotherm models: (a) Langmuir; (b) Freundlich.

The adsorption behavior of Fe(II) onto Rs-OCa was evaluated using both Langmuir and Freundlich isotherm models. The Langmuir plot of C_e/q_e versus C_e (**Figure 6(a)**) produced a linear regression equation of y=0.0445x+0.2921 with an R^2 value of 0.9997, indicating an almost perfect fit to the Langmuir model. From the intercept ($1/Q_m$) and slope ($1/(K_L \cdot Q_m)$, the maximum adsorption capacity (Q_m) was calculated as 22.47 mg/g, while the Langmuir constant (K_L) was determined to be 0.1539 L/mg. These parameters suggest that adsorption occurs on a homogeneous surface with uniform active sites, forming a monolayer coverage of Fe(II) ions, and that Rs-OCa exhibits strong binding affinity toward the target metal ion.In contrast, the Freundlich model, represented by the plot of log q_e versus log C_e (**Figure 6(b)**), the regression equation y=0.299x+0.8365 with an R^2 value of 0.9926, also demonstrating a strong correlation between the model and experimental data. The slope (1/n) of 0.299 corresponds to an adsorption intensity (n) of 3.34, indicating favorable adsorption, while the intercept (log K_F) of 0.8365 gives a Freundlich constant (K_F) of 6.85 mg/g(L/mg)$^{1/n}$, signifying considerable adsorption capacity at lower Fe(II) concentrations. These results imply that the Rs-OCa surface is heterogeneous, with active sites of varying affinities that can facilitate multilayer adsorption. Although both models fit the experimental data well, the higher R^2 value for the Langmuir model confirms that the adsorption process predominantly follows a monolayer mechanism on a relatively uniform surface. Nevertheless, the Freundlich parameters reveal that surface heterogeneity plays a role in adsorption at lower concentrations, providing complementary insight into the adsorption mechanism. This dual-model analysis underscores the high adsorption performance and versatility of Rs-OCa as an efficient and cost-effective adsorbent for Fe(II) removal from aqueous systems.

4. Conclusion

This study successfully demonstrated the synthesis and application of calcium hydroxide-modified rice straw (Rs-OCa) as a novel, low-cost, and eco-friendly adsorbent for Fe(II) removal from aqueous solutions. The modification process significantly enhanced the physicochemical properties of raw rice straw, as evidenced by FTIR and XRD analyses, which revealed the introduction of additional functional groups and structural changes that improved adsorption performance.The adsorption experiments confirmed that Rs-OCa

performs optimally at pH 4–5 and an adsorbent dosage of 0.75–1.0 g per 100 mL, with a maximum adsorption capacity of 22.47 mg/g as described by the Langmuir isotherm model. Kinetic analysis indicated that the adsorption process follows a pseudo-second-order model, suggesting a chemisorption mechanism involving electrostatic attraction and surface complexation with active sites such as hydroxyl (-OH) and carboxyl (-COOH) groups. The novelty of this research lies in the conversion of underutilized agricultural waste—rice straw—into a chemically activated adsorbent using $Ca(OH)_2$. This approach not only offers an efficient method for Fe(II) removal but also contributes to environmental sustainability by reducing biomass waste and utilizing an abundant, renewable resource. Furthermore, the study achieves its objective by demonstrating that the synthesized Rs-OCa is effective, scalable, and suitable for treating Fe-contaminated water, especially in rural or low-resource settings where conventional treatment methods may be costly or inaccessible. The ability of Rs-OCa to function under mild operational conditions and its compatibility with natural water systems underscores its potential as a viable solution for practical water treatment applications. Future research should therefore investigate the performance of Rs-OCa in multi-component systems that mimic the composition of natural groundwater. Furthermore, strategies such as pre-filtration to remove suspended solids, or selective surface modifications to enhance preferential binding toward Fe(II) ions over other cations, could be explored to improve the robustness and selectivity of Rs-OCa in practical water treatment applications. Evaluating the adsorbent's reusability and resistance to fouling under realistic conditions will also be crucial to ensuring its viability for field deployment.

Akcnowledgment

The authors gratefully acknowledge the support from the Directorate of Research, Technology, and Community Service, Directorate General of Higher Education, Research, and Technology, Ministry of Education, Culture, Research, and Technology of the Republic of Indonesia, through the Fundamental Research scheme for the 2025 fiscal year (Contract Number: 089/C3/DT.05.00/PL/2025).

Author contributions

Concept and Supervision: Nur Qudus, Harianingsih. Data Collection: Indra Sakti Pangestu, Rizky Ilham Fadzillah, Manuscript Writing: Dimas Gustoro, Muhammad Arief Kariem. Proofreading: Virgiawan Adi Kristianto.

Conflict of interest

The authors declare no conflict of interest.

References

1. Xu F, Li P. Biogeochemical mechanisms of iron (Fe) and manganese (Mn) in groundwater and soil profiles in the Zhongning section of the Weining Plain (northwest China). Science of The Total Environment 2024; 173506. https://doi.org/10.1016/j.scitotenv.2024.173506.
2. Lee WS, Aziz HA, Akbar NA, Wang MHS, Wang LK. Removal of Fe and Mn from groundwater. In: Industrial Waste Engineering. Cham: Springer International Publishing 2024; 135-170. https://doi.org/10.1007/978-3-031-46747-912.
3. Zhang R, Leiviskä T, Tanskanen J, Gao B, Yue Q. Utilization of ferric groundwater treatment residuals for inorganic-organic hybrid biosorbent preparation and its use for vanadium removal. Chemical Engineering Journal 2019; 361: 680-689. https://doi.org/10.1016/j.cej.2018.12.122.
4. Zhang YU, Yang MIN, Dou XM, He H, Wang DS. Arsenate adsorption on an Fe−Ce bimetal oxide adsorbent: role of surface properties. Environmental Science & Technology 2005; 39(18): 7246-7253. https://doi.org/10.1021/es050775d.
5. Bhatnagar A, Sillanpää M. Removal of natural organic matter (NOM) and its constituents from water by adsorption–a review. Chemosphere 2017; 166: 497-510. https://doi.org/10.1016/j.chemosphere.2016.09.098.
6. Ewis D, Ba-Abbad MM, Benamor A, El-Naas MH. Adsorption of organic water pollutants by clays and clay minerals composites: A comprehensive review. Applied Clay Science 2022; 229: 106686. https://doi.org/10.1016/j.clay.2022.106686.

7. Swaren L, Safari S, Konhauser KO, Alessi DS. Pyrolyzed biomass-derived nanoparticles: a review of surface chemistry, contaminant mobility, and future research avenues to fill the gaps. Biochar 2022; 4(1): 33. doi: (if available). https://doi.org/10.1007/s42773-022-00152-3.
8. Bayuo J, Rwiza M, Mtei K. A comprehensive review on the decontamination of lead (II) from water and wastewater by low-cost biosorbents. RSC advances 2022; 12(18): 11233-11254. https://doi.org/10.1039/d2ra00796g.
9. Salem LR. Kinetics and adsorption isotherm of strontium on sugarcane biochar and its application in polluted soil. International Journal of Environmental Research 2023; 17(3): 42. https://doi.org/10.1007/s41742-023-00532-y.
10. Siswoyo E, Dai Y, Mori M, Wada N, Itabashi H. Environmentally Friendly Adsorbents. In: Design of Materials and Technologies for Environmental Remediation. Singapore: Springer Nature Singapore 2022; 293-333. https://doi.org/10.1007/698_2021_827.
11. Bambal A, Gomase V, Saravanan D, Jugade R. Highly efficient mesoporous aluminium-magnetite-alginate magnetic composite for defluoridation of water. Environmental Research 2024; 261: 119698. https://doi.org/10.1016/j.envres.2024.119698.
12. Zhang T, Payne K, Zhang J, Purswani P, Karpyn Z, Wang M. Hybrid ion exchange and biological processes for water and wastewater treatment: a comprehensive review of process applications and mathematical modeling. Reviews in Environmental Science and Bio/Technology 2024; 23(1): 163-188. https://doi.org/10.1007/s11157-023-09677-w.
13. Bhatia D, Saroha AK. Use of Iron-Modified Biochar Obtained from Rice Straw as an Adsorbent for Removal of Arsenic from Water. Journal of Hazardous, Toxic, and Radioactive Waste 2024; 28(3): 04024010. https://doi.org/10.1061/jhtrbp.hzeng-1304.
14. Khan BA, Ahmad M, Bolan N, Farooqi A, Iqbal S, Mickan B, et al. A mechanistic approach to arsenic adsorption and immobilization in aqueous solution, groundwater, and contaminated paddy soil using pine-cone magnetic biochar. Environmental Research 2024; 245: 117922. https://doi.org/10.1016/j.envres.2023.117922.
15. Akbari Zadeh M, Daghbandan A, Abbasi Souraki B. Removal of iron and manganese from groundwater sources using nano-biosorbents. Chemical and Biological Technologies in Agriculture 2022; 9: 1-14. https://doi.org/10.1186/s40538-021-00268-x.
16. Singh S, Saksham, Kaith BS, Kumar R, Bajwa BS, Kaur I. Nanocellulose extracted from wheat straw: facile synthesis, characterization and application as an efficient U (VI) scavenger for groundwater of Bathinda district, SW-Punjab. Journal of Radioanalytical and Nuclear Chemistry 2024; 333(6): 3229-3238. https://doi.org/10.1007/s10967-023-09314-4.
17. Senapati S, Giri J, Mallick L, Biswal P, Mohapatra S, Behera D, et al. Ultra-fast adsorption of the industrial cationic dye pollutant using nitric acid-activated rice straw biochar: insights into adsorption mechanisms. Biomass Conversion and Biorefinery 2025; 1-19. https://doi.org/10.1007/s13399-025-06540-6.
18. Dakhem M, Ghanati F, Afshar Mohammadian M, Sharifi M. Effective biosorption of Al ions from drinking water by lignocellulosic biomass rice straw. International Journal of Phytoremediation 2024; 26(7): 1087-1098. https://doi.org/10.1080/15226514.2023.2289588.
19. Smolyanichenko A. Physical and chemical properties of silver-containing nanosorbent obtained from rice straw biochar. Agriculture 2023; 13(7): 1288. https://doi.org/10.3390/agriculture13071288.
20. Hamid Y, Chen Y, Lin Q, Haris M, Usman M, Rashid MS, et al. Functionality of wheat straw-derived biochar enhanced its efficiency for actively capping Cd and Pb in contaminated water and soil matrices: Insights through batch adsorption and flow-through experiments. Chemosphere 2024; 362: 142770. https://doi.org/10.1016/j.chemosphere.2024.142770.
21. Nguyen TH, Pham TH, Nguyen Thi HT, Nguyen TN, Nguyen MV, Tran Dinh T, et al. Synthesis of Iron-Modified Biochar Derived from Rice Straw and Its Application to Arsenic Removal. Journal of Chemistry 2019; 2019(1): 5295610. https://doi.org/10.1155/2019/5295610.
22. Umare S, Thawait AK, Dhawane SH. Remediation of arsenic and fluoride from groundwater: a critical review on bioadsorption, mechanism, future application, and challenges for water purification. Environmental Science and Pollution Research 2024; 1-30. https://doi.org/10.1007/s11356-024-33679-y.
23. Huang H, Ge L, Zhang X, Chen H, Shen Y, Xiao J, et al. Rice straw biochar and lime regulate the availability of heavy metals by managing colloid-associated-but dissolved-heavy metals. Chemosphere 2024; 349: 140813. https://doi.org/10.1016/j.chemosphere.2023.140813.
24. Darma A, Liu Y, Xia X, Wang Y, Jin L, Yang J. Arsenic (III) sorption on organo-ferrihydrite coprecipitates: Insights from maize and rape straw-derived DOM. Chemosphere 2024; 352: 141372. https://doi.org/10.1016/j.chemosphere.2024.141372.
25. Robles-Jimarez HR, Sanjuan-Navarro L, Jornet-Martínez N, Primaz CT, Teruel-Juanes R, Molins-Legua C, et al. New silica based adsorbent material from rice straw and its in-flow application to nitrate reduction in waters: Process sustainability and scale-up possibilities. Science of the Total Environment 2022; 805: 150317. https://doi.org/10.1016/j.scitotenv.2021.150317.
26. Robles-Jimarez HR, Sanjuan-Navarro L, Jornet-Martínez N, Primaz CT, Teruel-Juanes R, Molins-Legua C, et al. New silica based adsorbent material from rice straw and its in-flow application to nitrate reduction in waters:

Process sustainability and scale-up possibilities. Science of the Total Environment 2022; 805: 150317. https://doi.org/10.1016/j.scitotenv.2021.150317.
27. Ha TTV, Viet NM, Quan VT, Huong NTL. Novel Fe3O4-modified biochar generated from rice husk: a sustainable strategy for strengthening lead absorption in wastewater. International Journal of Environmental Science and Technology 2024; 1-10. https://doi.org/10.1007/s13762-024-05626-4.
28. Haris M, Amjad Z, Usman M, Saleem A, Dyussenova A, Mahmood Z, et al. A review of crop residue-based biochar as an efficient adsorbent to remove trace elements from aquatic systems. Biochar 2024; 6(1): 47. https://doi.org/10.1007/s42773-024-00341-2.
29. Rani M, Keshu, Shanker U. Green synthesis of sunlight active rice husk biochar loaded with metal ferrite nanocomposite for efficient removal of pesticides: kinetics and photoactivity. Biomass Conversion and Biorefinery 2024; 1-15. https://doi.org/10.1007/s13399-024-06000-7.
30. Abed EA, Alaboudi KA, Abbas MH, Attia TM, Abdelhafez AA. Iron Contamination in Groundwater: Risk Assessment and Remediation Techniques in Egypt's New Valley. Water 2024; 16(13): 1834. https://doi.org/10.3390/w16131834.
31. Chatzimichailidou S, Xanthopoulou M, Tolkou AK, Katsoyiannis IA. Biochar derived from rice by-products for arsenic and chromium removal by adsorption: a review. Journal of Composites Science 2023; 7(2): 59. https://doi.org/10.3390/jcs7020059.
32. Pap S, Sekulic MT, Tran HN, Chao HP, Gilbert PJ, Gibb SW, et al. Comparison of two carbonaceous supported Fe-rich adsorbents for arsenate removal: A functionalisation and mechanistic study with applicability to groundwater treatment. Chemosphere 2024; 359: 142205. https://doi.org/10.1016/j.chemosphere.2024.142205.
33. Liang T, Zhou G, Chang D, Ma Z, Gao S, Nie J, et al. The dissolved organic matter from the co-decomposition of Chinese milk vetch and rice straw induces the strengthening of Cd remediation by Fe-modified biochar. Biochar 2024; 6(1): 27. https://doi.org/10.1007/s42773-024-00313-6.
34. Lee WS, Aziz HA, Akbar NA, Wang MHS, Wang LK. Removal of Fe and Mn from groundwater. In: Industrial Waste Engineering. Cham: Springer International Publishing 2024; 135-170. https://doi.org/10.1007/978-3-031-46747-9_4.
35. Mohiuddin I, Singh R, Kaur V. Blending polydopamine-derived imprinted polymers with rice straw-based fluorescent carbon dots for selective detection and adsorptive removal of ibuprofen. International Journal of Biological Macromolecules 2024; 269: 131765. https://doi.org/10.1016/j.ijbiomac.2024.131765.
36. Dakhem M, Ghanati F, Afshar Mohammadian M, Sharifi M. Effective biosorption of Al ions from drinking water by lignocellulosic biomass rice straw. International Journal of Phytoremediation 2024; 26(7): 1087-1098. https://doi.org/10.1080/15226514.2023.2289588.
37. Sakhiya AK, Vijay VK, Kaushal P. Development of rice straw biochar through pyrolysis to improve drinking water quality in arsenic and manganese contaminated areas. Surfaces and Interfaces 2023; 36: 102582. https://doi.org/10.1016/j.surfin.2022.102582.
38. Ning K, Chen H, Wang D, Hu Y, He Y, Hao S, et al. Effective removal of fluoride and lead ions from aqueous solutions using water treatment residue and rice straw co-pyrolysis biochar composites. Environmental Technology & Innovation 2024; 34: 103589. https://doi.org/10.1016/j.eti.2024.103589.
39. Umare S, Thawait AK, Dhawane SH. Remediation of arsenic and fluoride from groundwater: a critical review on bioadsorption, mechanism, future application, and challenges for water purification. Environmental Science and Pollution Research 2024; 1-30. https://doi.org/10.1007/s11356-024-33679-y.
40. Cuong VT, Nguyen TH, Do TX, Vu AT. Preparation of novel CS/SiO2-EDTA nanocomposite from ash of rice straw pellets for enhanced removal efficiency of heavy metal ions in aqueous medium. Journal of Water Process Engineering 2024; 60: 105175. https://doi.org/10.1016/j.jwpe.2024.105175.
41. Ahmad S, Gautam SB, Sawood GM, Dixit S, Mishra A. Modified paddy husk carbon with linked fibrils of FeHO2 using aluminium as the surface regulator for enhanced As (III) removal in fixed bed system. International Journal of Chemical Reactor Engineering 2024; 22(2): 153-170. https://doi.org/10.21203/rs.3.rs-3028579/v1.
42. Chowdhury MF, Khanum MUKH, Rahman MA, Rahman MM, Kabir SF, Rahaman MH, et al. Dynamic intercalation of methylene blue in BC-MgFe-HT composite: Unveiling adsorption mechanisms for efficient wastewater treatment. Groundwater for Sustainable Development 2024; 27: 101314. https://doi.org/10.1016/j.gsd.2024.101314.